CHEMICAL ENGINEERING TRANSACTIONS
VOL. 76, 2019
A publication of AIDIC
The Italian Association of Chemical Engineering
Online at www.aidic.it/cet
Guest Editors: Petar S. Varbanov, Timothy G. Walmsley, Jiří J. Klemeš, Panos Seferlis

ISBN 978-88-95608-73-0; **ISSN** 2283-9216
DOI: 10.3303/CET1976116

Modelling and Dynamic Behaviour Analysis of the Steam Supply System for Double-Reactor and Multi-Turbine Nuclear Power Plant

Chengcheng Cui, Jiong Shen*, Junli Zhang, Xiao Wu, Lei Pan

Key Laboratory of Energy Thermal Conversion and Control of Ministry of Education, School of Energy and Environment, Southeast University, Sipailou2, Nanjing Jiangsu Province, 2l0096
shenj@seu.edu.cn

This paper proposes a first principle dynamic model of the Nuclear Steam Supply System (NSSS) for the Double-Reactor and Multi-Turbine Nuclear Power Plant (DMNPP). The main devices within the nuclear steam supply system, such as Once Through Steam Generator (OTSG), Steam Main Pipe (SMP)and Steam Turbine (ST) are modelled using the movable boundary approach and discrete approximate distributed modelling method. Dynamic behaviour analysis is then carried out on the developed model, through which, the dynamic characteristics of key variables, such as the distribution pressures in the SMP are investigated in detail. The simulation results show that when the opening degree of the ST regulating valve or the OTSG steam valve change, the fluctuations of the pressure at each point in the SMP are different. The maximum fluctuation value of the pressure is 0.12 MPa when the opening degree of the third ST regulating valve is increased by 20 % and is 0.015 MPa when the opening degree of the second OTSG steam valve is increased by 10 %. It is discovered that the steam pressure of the SMP has a self-stabilizing ability and the NSSS of the DMNPP is of highly nonlinearity and strongly coupled among multi-variables.

1. Introduction

The pressures of the main steam in NSSS in DMNPP affect the safe and economic operation of the system. Developing a satisfactory dynamic model for the NSSS in the DMNPP and gaining in-depth knowledge of its dynamic behaviours are thus important to provide guidance for the operating control design.
The NSSS composed of four OTSGs, four STs and one SMP in the DMNPP is shown in Figure 1. The water in the OTSG absorbs the heat of the coolant in the primary circuit and is turned into the slightly superheated steam. The steam is sent to the SMP and then flows into the ST. The NSSS is the core part of the nuclear power plant.

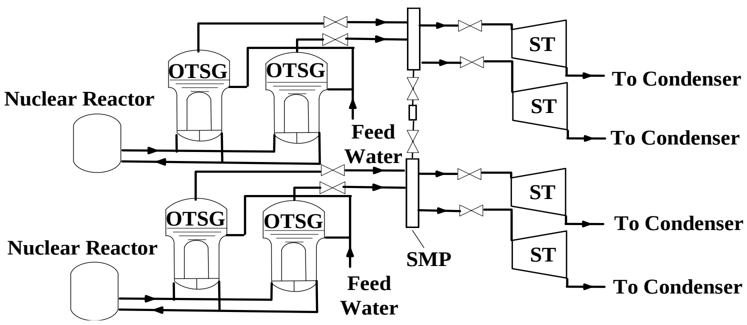

Figure 1: Diagram of the DMNPP

Paper Received: 16/03/2019; Revised: 19/06/2019; Accepted: 13/07/2019
Please cite this article as: Cui C., Shen J., Zhang J., Wu X., Pan L., 2019, Modelling and Dynamic Behaviour Analysis of the Steam Supply System for Double-Reactor and Multi-Turbine Nuclear Power Plant, Chemical Engineering Transactions, 76, 691-696 DOI:10.3303/CET1976116

Current modelling and dynamic studies on the NSSS mainly focused on a single equipment or the system with single reactor. Salehi et al., (2019) conducted the modelling and control work on the steam generator; Chen et al., (2019) developed a novel simulation method for the thermodynamic performance of a parallel dual-pressure OTSG under both design and off-design operating conditions; Cui et al., (2018) developed a secondary loop system model for the marine single-reactor nuclear power system, and the simulation results under various conditions showed that the secondary loop system had strong couplings among many thermal parameters; Dong et al., (2018) proposed a lumped-parameter dynamical model for the nuclear heating reactor cogeneration plant NHR200-II plant, which can be utilized for the control system design and the development of a real-time simulator; Nie et al., (2018) established a full-system simulation platform of the marine single-reactor nuclear power plant for the quantitative and qualitative analysis on the entire system. However, the NSSS of the nuclear power system composed with multiple reactors and turbines is more complicated and its dynamic behaviour cannot be simply approximated by the summation of several single-reactor nuclear power systems. Some studies have been carried out on the modelling and dynamic analysis of the NSSS in the multi-reactor nuclear power system. For example, Fang et al., (2016) developed the model of the DMNPP with the real-time RELAP5 program and the JTOPMERET program; Xiao et al., (2017) built the model of the same object using the RELAP5 program and the 3KEYMASTER program. While the steam main pipe in the above two was modelled as the lumped object, which ignored its distributed dynamic characteristic.
There are still very limited results for the modelling and dynamic characteristics of the NSSS in the multi-reactor nuclear power system. Motivated by the gap between the importance and the lack of results in this field, a dynamic model of the NSSS in the DMNPP is developed in this study. A discrete approximate distributed modelling method is used to build the model of the SMP in the NSSS innovatively in this paper, which can reflect its distributed dynamic characteristic well, which is vital for the dynamic analysis of the NSSS. The dynamic behaviours of key variables within the NSSS are then analysed based on the model.

2. The model of the NSSS

The NSSS is divided into OTSG module, SMP module and ST module, and the dynamic models of the three modules are developed respectively through the MATLAB/SIMULINK platform. The OTSG and the SMP are modelled through the movable boundary approach and the discrete approximate distributed modelling method (DADMM) respectively, and the ST is modelled through the lumped parameter method.

2.1 The mathematical model of the OTSG

The following assumptions are made: (1) OTSG is set as one straight flow channel. (2) Neglecting the axial heat conduction of the tube wall and the fluid. (3) The enthalpy and temperature vary linearly in each region. (4) One-dimensional flows in primary side and secondary side. (5) Homogeneous heat flux in each region. (6) Steady-state model for primary circuit heat transfer. These assumptions are reasonable for the fact that the flow state in each tube of the OTSG is almost the same, and that the axial heat conduction is so small compared to radial heat transfer that it can be ignored.
According to the characteristics of the water in the secondary circuit, the OTSG can be divided into subcooled region, two-phase region and superheated region (as shown in the Figure 2), and the boundaries of them are movable. In the Figure 2, node 3 and node 5 are saturated water point and saturated steam point. Node 1 and node 7 represent the inlet of the subcooled region and the outlet of the superheated region; node 2, node 4 and node 6 are the average points in each region. l_{17} is the total length of the tube in the OTSG, and it is a fixed value; l_{13}, l_{35} and l_{57} are the lengths of subcooled region, two-phase region and superheated region. The subscript 's' represents the secondary side, 'p' represents the primary side, and 'm' represents the tube wall.

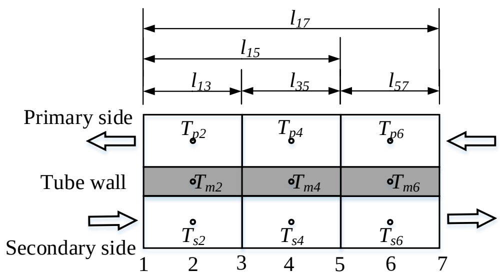

Figure 2: Diagram of the three regions of the OTSG

(1) Equations of the secondary side

The basic conservation equations of mass, energy, and momentum according to the abovementioned basic assumptions can be expressed as follows:

$$\left.\begin{aligned}\frac{\partial\rho}{\partial t}&=-\frac{\partial\left(G/A_{cs}\right)}{\partial l}\\ \frac{\partial(\rho h)}{\partial t}&=-\frac{\partial\left(Gh/A_{cs}\right)}{\partial l}+\frac{q}{A_{cs}}+\frac{\partial p}{\partial t}\\ \frac{\partial\left(G/A_{cs}\right)}{\partial t}&=-\frac{\partial}{\partial l}\left(\frac{\left(G/A_{cs}\right)^2}{\rho}\right)-\frac{\partial p}{\partial l}+r\end{aligned}\right\} \tag{1}$$

where t is the time (s). l is the length (m). ρ is the fluid density (kg/m^3). G is the fluid mass flow rate (kg/s). h is the fluid enthalpy per unit mass (J/kg). q is the thermal flux per unit length (W/m). p is the pressure (Pa). A_{cs} is the cross-section area of the secondary side (m^2). r is the pressure drop per unit length (Pa/m). Assuming that the pressure drop in each region is concentrated at the inlet of the pipe (This is a common assumption used for the pipe pressure), so $p_{s4} = p_{s5}$. Integrate the mass and energy equations with length in two-phase region and combine them, and the result is as follow:

$$\begin{aligned}&\left[\rho_{s3}\left(h_{s3}-h_{s4}\right)+\left(p_{s5}-p_{s3}\right)\right]\frac{dl_{13}}{dt}+\rho_{s5}\left(h_{s4}-h_{s5}\right)\frac{dl_{15}}{dt}+\frac{l_{35}}{2}\rho_{s4}\frac{\partial h_{s3}}{\partial p_{s3}}\frac{dp_{s3}}{dt}+\frac{l_{35}}{2}\left(\rho_{s4}\left.\frac{\partial h_{s5}}{\partial p_{s5}}\right|_{p_{s5}}-2\right)\frac{dp_{s5}}{dt}\\&=\frac{G_{s5}\left(h_{s4}-h_{s5}\right)}{A_{cs}}+\frac{G_{s3}\left(h_{s3}-h_{s4}\right)}{A_{cs}}+\frac{Q_{s4}}{A_{cs}}\end{aligned} \tag{2}$$

Where $G_{s4} = (G_{s3} + G_{s5})/2$, $h_{s4} = (h_{s3} + h_{s5})/2$. The average density of the vapor-liquid mixed phase in the two-phase region can be obtained from the Eq. (3):

$$\rho_{s4}=a\rho_{s5}+(1-a)\rho_{s3} \tag{3}$$

where a is the void fraction, a = x*γ/(1 + x*(γ - 1)), $\gamma = 1.5\,(\rho_{s3}/\rho_{s5})^{0.692-0.5}$. After the simplification, integration and derivation, the momentum equation in the two-phase region can be expressed as:

$$\frac{dp_{s5}}{dt}=\frac{dp_{s3}}{dt}+F_{s4}G_{s4}^2/A_{cs}^2\frac{dl_{13}}{dt}-F_{s4}G_{s4}^2/A_{cs}^2\frac{dl_{15}}{dt}-\frac{2F_{s4}G_{s4}l_{35}}{A_{cs}^2}\frac{dG_{s3}}{dt} \tag{4}$$

where F_{s4} is the friction coefficient in two-phase region (Liew et al., 2014). The same method is used in the other two regions.

(2) Equations of the primary side

The steady-state model is used in the primary side for the heat transfer. Assuming that the flow rate of the water in the primary side remains unchanged, the energy equations in the three regions are as follows:

$$\left.\begin{aligned}c_pG_p\left(T_{p3}-T_{p1}\right)&=A_{p2}\alpha_{p2}\left(T_{p2}-T_{m2}\right)\\ c_pG_p\left(T_{p5}-T_{p3}\right)&=A_{p4}\alpha_{p4}\left(T_{p4}-T_{m4}\right)\\ c_pG_p\left(T_{p7}-T_{p5}\right)&=A_{p6}\alpha_{p6}\left(T_{p6}-T_{m6}\right)\end{aligned}\right\} \tag{5}$$

where c_p is the specific isobaric heat capacity of the water (J/(kg ℃)). α_p is the convection heat transfer coefficient in the primary side (W/(m^2.℃))

(3) Equations of the tube wall

The heat balance equations of the tube wall in the three regions are as follows:

$$\left.\begin{aligned}\frac{dT_{m2}}{dt}&=\frac{Q_{p2}-Q_{s2}}{A_{m2}\rho_{m2}c_{m2}l_{13}}+\frac{T_{m4}-T_{m2}}{l_{15}}\frac{dl_{13}}{dt}\\ \frac{dT_{m4}}{dt}&=\frac{Q_{p4}-Q_{s4}}{A_{m4}\rho_{m4}c_{m4}\left(l_{15}-l_{13}\right)}+\frac{T_{m4}-T_{m2}}{l_{15}}\frac{dl_{13}}{dt}+\frac{T_{m6}-T_{m4}}{l_{17}-l_{13}}\frac{dl_{15}}{dt}\\ \frac{dT_{m6}}{dt}&=\frac{Q_{p6}-Q_{s6}}{A_{m6}\rho_{m6}c_{m6}\left(l_{17}-l_{15}\right)}+\frac{T_{m6}-T_{m4}}{l_{17}-l_{13}}\frac{dl_{15}}{dt}\end{aligned}\right\} \tag{6}$$

where c_m is the specific heat of tube wall (J/(kg ℃)). Q_p is the heat transferred from the primary side to the tube wall (W), and $Q_p = A_p*\alpha_p(T_p - T_m)$. Q_s is the heat transferred from tube wall to the secondary side (W), and $Q_s = A_s*\alpha_s(T_m - T_s)$. α_s is the convection heat transfer coefficient in the secondary side (W/(m^2.℃)). The Seder-Tate formula is used to calculate heat transfer coefficients of the primary side and heat transfer coefficients of the subcooled region and superheated region of the secondary side. Chen formula is used for the heat transfer coefficient of the two-phase region of the secondary side (Zhao et al., 1992).

2.2 The mathematical model of the SMP

The model of the SMP is developed through the DADMM, in which the SMP is divided into several short segments by the access points of the OTSGs and the STs (shown in the Figure 3). Assuming that the resistance in each short pipe is concentrated in the middle of the pipe section (For each short segment of the SMP, this assumption is reasonable when it is considered as a lumped object), the pipe section between two adjacent resistance links is regarded as a lumped parameter object. The influence of the relative position of the OTSG and the ST on the distributed pressures in the SMP is considered in this method and the distributed dynamic characteristics of the SMP are reflected.

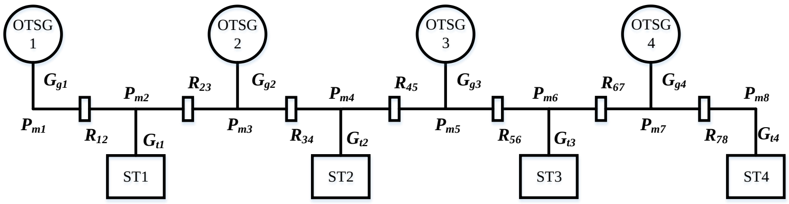

Figure 3: Diagram of the segmentation in SMP

Taking the pipe section connected with an OTSG as an example and assuming that the flowing of the steam in SMP is constant and adiabatic (The heat loss of the steam is small and negligible in the SMP). The total steam flow rate of the pipe i can be expressed as follows:

$$\left.\begin{aligned} &\Delta G_i = dG_{(i-1)i} + dG_{(i+1)i} + G_{gj} \\ &dG_{(i-1)i} = \left(P_{\mathrm{m}(i-1)} - P_{\mathrm{m}i}\right)\big/R_{(i-1)i} \\ &dG_{(i+1)i} = \left(P_{\mathrm{m}(i+1)} - P_{\mathrm{m}i}\right)\big/R_{i(i+1)} \end{aligned}\right) \tag{7}$$

Where P_{mi} is the pressure of the pipe i (i = 1,2, …8) (Pa). $R_{i(i+1)}$ is the resistance link between the pipe sections. ΔG_i is the steam flow rate of the pipe i (kg/s). G_{gj} is the steam flow rate of the OTSG j (j = 1,2,3,4) (kg/s). The sign of the OTSG flow rate is positive, and that of the ST flow rate is negative.
Considering that the dynamic process of the pressure-flow channel is faster than that of the enthalpy-temperature channel, and that the influence of the temperature change on the steam storage in the link is small generally, the model of the pressure-flow channel of the pipe i is as follow ($C_{Mi} = V_i{*}d\rho_i/dP_{mi}$):

$$\Delta G_i = C_{Mi}\frac{dP_{mi}}{dt} \tag{8}$$

Similarly, the model of enthalpy-temperature channel of the pipe i can be obtained from the energy conservation, and the expression is as follow:

$$\frac{dh_i}{dt} = \frac{\sum G_{i\_in} h_{i\_in} - \sum G_{i\_out} h_i - C_{Mi} \mathrm{h}_i \dfrac{dP_{mi}}{dt}}{\rho_i V_i} \tag{9}$$

Where G_{i_in} and G_{i_out} are the mass flow rate (kg/s) that flows into and flows out of the pipe i; h_i is the enthalpy per unit mass of the steam in the pipe i (J/kg); h_{i_in} is the enthalpy per unit mass of the steam that flows into the pipe i (J/kg).

2.3 The mathematical model of the ST

The flow rate of the ST is determined by the pressure in the SMP, the back pressure of the ST and the opening degree of the ST regulating valve. The back pressure of the ST is small mostly, and its change has little influence on the flow rate of the ST. Assuming that the ST regulating valve is linear (The characteristics of the SMP can be better demonstrated based on this assumption), the flow rate of the ST can be expressed as follow:

$$G_t = \frac{1}{R_T} P_m + K_T \mu_T \tag{10}$$

Where G_t is the mass flow rate of the ST (kg/s). P_m is the pressure in the SMP (MPa). R_T is the flow resistance coefficient of the ST (MPa/(kg/s)). μ_T is the opening degree of the ST regulating valve. K_T is the static amplification factor of the ST regulating valve.

3. Simulation and results

The steady-state operating parameters of the NSSS are given in Table 1.

Table 1: Main parameters under the steady-state condition

G_{g1}/(kg/s)	G_{g2}/(kg/s)	G_{g3}/(kg/s)	G_{g4}/(kg/s)	G_{t1}/(kg/s)	G_{t2}/(kg/s)	G_{t3}/(kg/s)	G_{t4}/(kg/s)
106.4	106.4	106.4	106.4	109.6	107.5	105.3	103.2
P_{m1}/(MPa)	P_{m2}/(MPa)	P_{m3}/(MPa)	P_{m4}/(MPa)	P_{m5}/(MPa)	P_{m6}/(MPa)	P_{m7}/(MPa)	P_{m8}/(MPa)
6.114	5.890	5.897	5.680	5.689	5.475	5.481	5.265

Case 1. The first case is developed to investigate the dynamic behavior of the NSSS under regulating valve opening. The regulating valve opening of the third ST is increased from 50 % to 70 % at 150 s, and its influences on the main variables of the NSSS are shown in Figure 4. As the flow rate of the third ST is increased, the pressures at each measuring point in the SMP are reduced. Then the flow rates of the four OTSGs are increased for the pressure difference between the two sides of the steam valve is increased. The fluid temperatures at the outlet of the secondary side and the primary side of the four OTSGs are all reduced, resulting in the reduction of the steam enthalpy in the SMP. With the readjustment of the flow rate of each equipment near the disturbance source, the farther away from the third ST, the smaller the variation of the parameters. The flow rates of the other three STs are reduced for the pressure differences between the two sides of the regulating valves are reduced. In the initial stage of the change, there is a reverse change of the temperature and enthalpy in (d), (e), (f), for the reduction of the pressure is earlier than the increase of the flow rate in the OTSG.

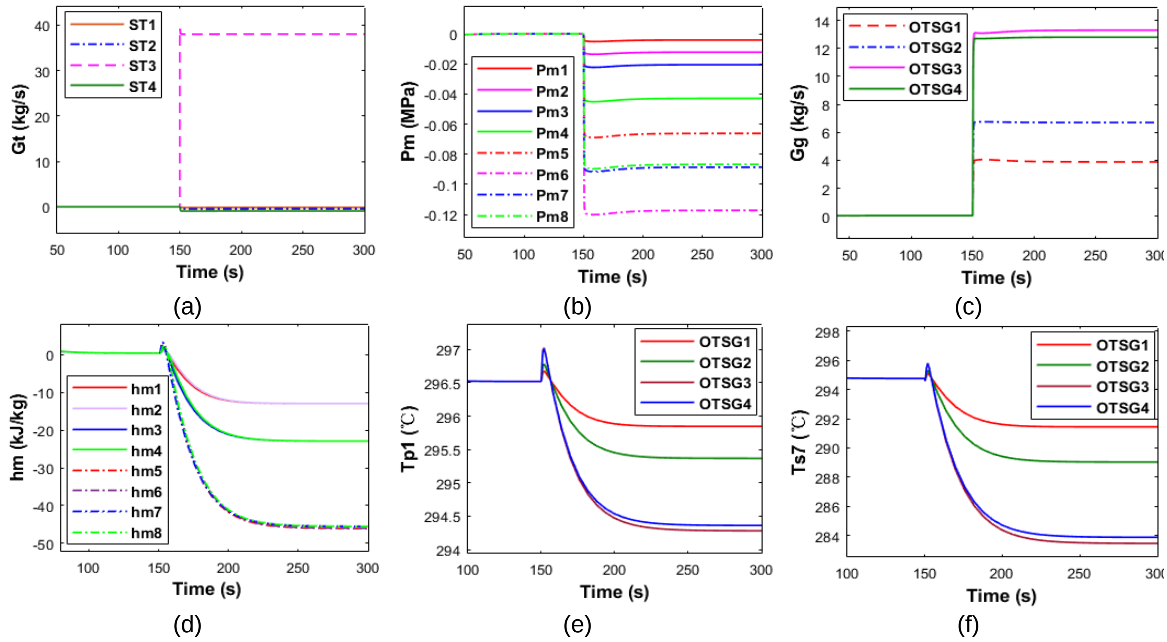

Figure 4: Response of main parameters due to the 20 % step-up in regulating valve opening of the third ST

Case 2. The second case is developed to investigate the dynamic behavior of the NSSS under steam valve opening of the OTSG. The steam valve opening of the second OTSG is increased from 50 % to 60 % at 150 s, and its influences on the main variables of the NSSS are shown in Figure 5. The flow rate of the second OTSG is increased. The fluid temperatures at the outlet of the secondary side and the primary side are increased in the other three OTSGs, and the steam enthalpies in the SMP near this three OTSGs are increased. The distributed pressures in the SMP and the flow rates of the STs are increased. The variations of the parameters in the system are inversely proportional to the distance from the disturbance source. The mechanism of the change is the same as that of the regulating valve opening disturbance for the ST.

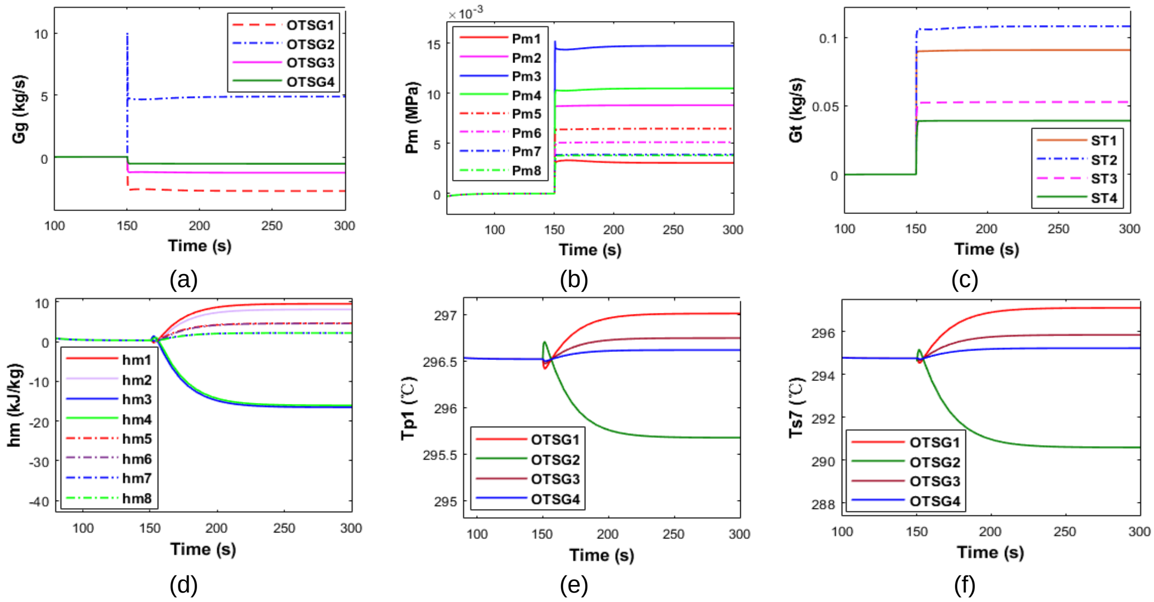

Figure 5: Response of main parameters due to the 10 % step-up in steam valve opening of the second OTSG

4. Conclusions

A dynamic model of the NSSS is developed in this paper and the effects of the ST valves and the OTSG steam valves on the key parameters are studied. The simulation results show that the fluctuations of pressure at each measuring point in the SMP are different under the disturbances, and the maximum fluctuation value is 0.12 MPa under the 20 % step-up in regulating valve opening of the third ST, and is 0.015 MPa under the 10 % step-up in steam valve opening of the second OTSG, which present the distributed feature of the SMP. The NSSS in DMNPP is of highly nonlinearity and has strong couplings among multi-variables. The steam pressures in the SMP can be stabilized on a new level after the disturbances. The flow redistribution in the system follows the "proximity principle" which should be considered in the distribution of the load.

Acknowledgments

This work was supported by the National Natural Science Foundation of China under Grant 51876036 and the Fundamental Research Funds for the Central Universities.

References

Chen Y.Z., Li Y.G., Newby M., 2019, Performance Simulation of a Parallel dual-pressure once-through steam generator, Energy, 173, 16-27.

Cui J., Yang Z., Zhang L., 2018, Thermodynamic Calculation Method and Characteristic Analysis of Marine Secondary Circuit System in full Operating Conditions. Chinese Journal of Ship Research, 13(2), 116-122.

Dong Z., Pan Y., 2018, A Lumped-parameter Dynamical Model of a Nuclear Heating Reactor Cogeneration Plant, Energy, 145, 638-656.

Fang M., 2016, Study on Operation Characteristics of Nuclear Power Plant with Multi-reactors, Harbin, China.

Liew P.Y., Wan Alwi S.R.W., Klemeš J.J., 2014, Total Site Heat Integration Targeting Algorithm Incorporating Plant Layout Issues, Computer Aided Chemical Engineering, 34, 1801-1806.

Nie W., Fang W., 2018, Research on Emulation Analysis for System Performance of Marine Nuclear Power Plant, Ship Science and Technology, 40(1), 94-98.

Salehi A., Safarzadeh O., Kazemi M. H., 2019, Fractional Order PID Control of Steam Generator Water Level for Nuclear Steam Supply Systems, Nuclear Engineering and Design, 342, 45-59.

Xiao K., Liao L., Zhou K., Chen Z., 2017, The Modelling and Simulation Research on Control Scheme of Multi-reactor and Multi-turbine Nuclear Power Plant, Journal of the University of South China (Natural Science), 31(3), 13-20.

Zhao Z., Zhu R.,1992, Reactor Thermal Fluid Dynamics, Beijing, China: Tsinghua University Press.